GOSPODARKA SUROWCAMI MINERALNYMI – MINERAL RESOURCES MANAGEMENT

2021 Volume 37 Issue 4 Pages 133–152

DOI: 10.24425/gsm.2021.139742

FENG JIN[1], KAI ZHAN[2], SHENGJIE CHEN[3], SHUWEI HUANG[4], YUANSHENG ZHANG[5]

Image segmentation method of mine pass soil and ore based on the fusion of the confidence edge detection algorithm and mean shift algorithm

Introduction

In metal mines, the ore on the grid sieve of the winze usually requires workers to manually control the crusher. In recent years, with the continuous development of automatic control technology, remote control technology through video surveillance combined with network transmission has gradually matured, make remote control technology a practical solution in some metal mines. In the process of guiding the crusher to crush the ore above the grid sieve of the winze, usually after the mine truck is unloaded, ore and finely divided ore deposits appear above the winze at the same time. At this time, if the crusher is guided to crush the fine ore, the front end of the crusher does not work effectively and the level of force required

✉ Corresponding Author: Shuwei Huang; e-mail: shuwei.huang@hotmail.com
[1] BGRIMM Technology Group; University of Science and Technology Beijing; China; ORCID iD: 0000-0003-3978-4984; e-mail: jinfeng@bgrimm.com
[2] BGRIMM Technology Group; China; e-mail: zhankai@163.com
[3] BGRIMM Technology Group; China; e-mail: chenshengjie@163.com
[4] BGRIMM Technology Group; China; e-mail: shuwei.huang@hotmail.com
[5] BGRIMM Technology Group; China; e-mail: zhangyuansheng@163.com

for crushing is not reached. This results in a large amount of finely divided ore accumulating above the grid sieve, and even after several attempts, the pile of small pieces of ore does not drop. At this point, it can be seen that for small pieces of ore, the crushing guidance cannot be carried out effectively, instead the crusher should be guided to disperse it. Therefore, for the image processing problem in the unattended remote fixed crushing process, the use of industrial cameras to obtain the RGB image of the ore above the winze is crucial. There is an urgent need for an efficient and accurate image segmentation algorithm (Qin and Liu 2015; Boyuan et al. 2021; Xu et al. 2019; Liu et al. 2020) to segment the ore or ore pile above the grid sieve of the winze, and then correctly guide the crusher to crush or disperse it.

In previous studies, commonly used ore image segmentation methods include watershed algorithms, graph theory-based methods, dynamic gray-scale threshold algorithms (Xu et al. 2019), region-based methods, convolutional neural network-based deep learning algorithms (Liu et al. 2020), and so on. Among these, the watershed algorithm (Qin and Liu 2015; Boyuan et al. 2021) belongs to the traditional image segmentation algorithm, the main principle of which is to perform segmentation through use of the gradient image. Due to the image noise, the segmentation result is over-segmented. Therefore, in many studies, various improved algorithms are proposed to solve the over-segmentation problem. Qin and Liu (2015) and others combine the labeling with the watershed algorithm which first executes the image preprocessing operation to fully eliminate the noise, then modifies the function of the segmentation algorithm, and finally segments the image. But the segmentation result still has the problem of over-segmentation when the noise distribution is obvious. For the research direction of using the dynamic gray threshold method to segment the ore, Xu et al. (Xu et al. 2019) and others proposed using the dual-window Otsu algorithm based on binomial distribution optimization. First, according to the idea of Otsu, the largest class of pixels in the field is divided into two categories. The window threshold is determined over time, and then two neighborhood windows are selected according to the target characteristics, and Otsu was applied to each window to calculate the best binarization threshold. Finally, the binarization method was used to obtain the target area from the background. This method only uses the dynamic gray threshold to perform binarization to complete the classification of the stone and the background, and does not perform independent segmentation for individual ores. In recent years, deep learning methods have been applied in various fields of computer vision, such as image classification and image segmentation. Liu et al. (Liu et al. 2020) and others proposed using U-Net combined with the UR method of Res-Unet to segment ores. Before using the UR method, image preprocessing, model training, test training and other processes are required. This method will have a better segmentation result on ore scenes with clear boundaries and less overlap, but the segmentation result of the mixed ore and ore piles is not good. In summary, it can be seen that the current image segmentation algorithms applied in ore images have some drawbacks and shortcomings. It is necessary to propose a more effective algorithm, which can not only solve the over-segmentation problem of the watershed algorithm but can also independently segment the ore and ore pile region with very similar colors and textures in the mixed scene of ore and ore piles.

In this regard, this paper proposes to use the edge information of the image to distinguish the types of ore and ore pile (Lin et al. 2005; Comaniciu and Meer 1997; Koschan 1994). This involves first using the edge distribution around the segmented area to determine whether the image area is ore or ore pile. This is followed by combining the position relationship of the camera coordinate of the 2D camera and the 3D camera to find the three-dimensional data information corresponding to the final segmented region and transmitting the three-dimensional data to the crusher control system to guide the crusher to complete the crushing action. This begins with use of the image segmentation algorithm based on mean shift (Xiang-Ru et al. 2005; Comaniciu and Meer 1999; Georgescu et al. 2003; Cheng 1995; Comaniciu and Meer 2002) to initially segment the ore region and then use the edge detection algorithm based on confidence (Ying et al. 2005) to merge the segmented sub-image regions and then achieve a better ore or ore area segmentation result. The second stage is to calibrate the coordinate system of the 2D industrial camera and the 3D stereo camera to obtain the position relationship between the two cameras and then obtain the 3D data corresponding to the RGB single pixel or the image point sets, and finally to guide the crusher to crush or disperse.

In the entire remote-control crushing process, the first stage of image segmentation is very important, which is the main research subject of this article. The first section of this article mainly introduces the principle of non-parametric density estimation based on sample points and the mean shift algorithm, and discusses kernel function and the procedure of the mean shift algorithm. The second section mainly introduces an edge detection algorithm based on confidence, gives the definition of confidence, and introduces two implementation methods of edge detection, namely non-maximum suppression and hysteresis threshold processing. Finally, the strategy of parameter selection is given. The third section introduces the steps of fusing the mean shift segmentation algorithm and the edge detection algorithm based on confidence to merge the over-segmentation region of the initial segmented result. The idea is that after the initial clustering segmentation, there are lots of over-segmentation ore regions, that is to say, a complete piece of ore is divided into multiple small areas. Using the distribution of edge points around the boundary of the ore region, it is judged whether the ore region should be merged. In the fourth section, the ore is set above the grid sieve of the winze as the experimental object, and the initial segmentation area is merged with the surrounding segmentation area by using the methods of the previous three sections to obtain the final merged area. The proportion of the merged region to the actual ore region is then analyzed.

1. Mean shift algorithm image segmentation

1.1. Nonparametric estimation

The mean shift algorithm is mainly used in the feature space to find the local maximum point of the probability density function through continuous statistical iteration. The density function gradient is used for non-parametric estimation, and the density estimation of the final overall data set is obtained by derivation. Prior knowledge is not highly involved in the non-parametric estimation process, and it can be effectively estimated for sample data sets of any shape. The most commonly used method is kernel density estimation, which calculates the density function based on the kernel function $K(x)$ on the sample set. For each sample point x_i, a positive definite matrix Σ_i is used to represent the window shape and relative scale at x_i.

If the function $k(x)$ is non-negative in $[0,\infty)$ monotonically decreasing, and $\int_0^{+\infty} k(x) < +\infty$, then $k(x)$ is called a kernel function. Commonly used kernel functions, such as Gaussian kernel functions, usually have finite derivatives in each data domain and have non-increasing characteristics. Kernel estimation of sample point x_i for the overall data set is shown in Formula (1).

$$f\left(x \mid x_i\right) = K_i\left(x\right) = c_{k,i,h} k\left(\left(x - x_i\right)^T \Sigma_i^{-1}\left(x - x_i\right) / h^2\right) \tag{1}$$

Where $h > 0$ is used to adjust the window size from the overall perspective, and

$$c_{k,i,h} = \frac{1}{\int k\left(\left(x - x_i\right)^T \Sigma_i^{-1}\left(x - x_i\right) / h^2\right) dx} \tag{2}$$

Its main purpose is to ensure that $K_i(x)$ is a density function. If w_i is used to represent the prior probability of the occurrence of x_i, then the density of the overall X is estimated to be $\hat{f}(x) = \sum_{i=1}^{n} w_i K_i(x)$, and the condition is $\sum_{i=1}^{n} w_i = 1,, w_i > 0$.

H_i and $\left\|x - x_i\right\|_{H_i}^2$ as shown in Formula (3) and Formula (4) is convenient for subsequent expressions.

$$H_i = \frac{\sum_i^{-1}}{h^2} \tag{3}$$

$$\left\|x - x_i\right\|_{H_i}^2 = \left(x - x_i\right)^T H_i \left(x - x_i\right) \tag{4}$$

Then we can get

$$\hat{f}(x)=\sum_{i=1}^{n} w_i K_i(x)=\sum_{i=1}^{n} w_i c_{k,i,h} k\left(\left\|x-x_i\right\|_{H_i}^2\right) \tag{5}$$

The first step of the feature space analysis is to find patterns that satisfy this density function. These are usually located in the zero point of the gradient of the density function. Define the function $g(x) = -k'(x)$ in the above formula and define another kernel function at the same time, in the form of Formula (6).

$$G(x)=c_{g,d}\, g\left(\left\|x-x_i\right\|^2\right) \tag{6}$$

The gradient density can be obtained from the linearity of the density function, as shown in Formula (7).

$$\hat{\nabla} f_{H,K}(X)=\frac{2}{n}\left[\sum_{i=1}^{n} h_i^{d+2} g\left(\left\|\frac{X-X_i}{h_i}\right\|^2\right)\right]\left[\frac{\sum_{i=1}^{n}\frac{X_i}{h_i^{d+2}} g\left(\left\|\frac{X-X_i}{h_i}\right\|^2\right)}{\sum_{i=1}^{n}\frac{1}{h_i^{d+2}} g\left(\left\|\frac{X-X_i}{h_i}\right\|^2\right)}-X\right] \tag{7}$$

Formula (8) is expressed as a mean shift vector. When $h_1 = h_2 = ... = h_d$, as shown in Formula (9).

$$M_{h,G}(x)=\frac{\sum_{i=1}^{n} x_i g\left(\left\|\frac{x-x_i}{h}\right\|^2\right)}{\sum_{i=1}^{n} g\left(\left\|\frac{x-x_i}{h}\right\|^2\right)}-x \tag{8}$$

$$M_{h,g}(x)=\frac{1}{2}h^2 c\frac{\hat{\nabla} f_{h,g(X)}}{\hat{f}_{h,K(X)}} \tag{9}$$

When the mean shift algorithm is used to segment an image, the first step is to convert image pixels into sample points in the feature space. Following this is the implementation of the mean shift clustering algorithm on the collection of samples points. Through continuous iteration, all candidate mode points with the maximum local gradient density are found.

1.2. Image segmentation

Set $\{x_i\}_{i=1,...,n}$ as the initial sample point, and $\{z_i\}_{i=1,...,k}$ as the cluster mode points, and $\{L_i\}_{i=1,...,k}$ as the classification set. The steps of segmentation are as follows:

1) Feature extraction

With regard to the spatial characteristics and color characteristics of the image, the spatial characteristics take into account the pixel position information in the image space. The color characteristics can be divided into two parts: lightness and chroma. Since human vision is very sensitive to the *LUV* color space, we choose this color space as the feature space in this article. Among them, *L* represents brightness, and *U*,*V* component represents chromaticity parameters. Firstly, the value of *LUV* is calculated for all pixels in the color image to form the color feature and the coordinates of each pixel in the image are then obtained to form the spatial feature (*x**,*y**). The combination of spatial features and color features are used to form the sample points of pixels in the feature space, as shown in Equation (10).

$$x = (x^r, y^s) = (x^*, y^*, L, U, V) \tag{10}$$

2) Selection of kernel function

The multivariate kernel function $K(x)$ can be obtained by multiplying univariate kernel functions, that is $K(x) = \prod_{i=1}^{d} k_i(x_i)$, where x_i is the component of d-dimensional variable x. Since the color feature space and the spatial feature space are not related to each other, this paper uses a multivariate kernel function K_{h_s,h_r} to estimate the distribution of the sample point set, and K_{h_s,h_r} can be expressed as Formula (11).

$$K_{h_s,h_r}(x) = \frac{c}{h^2 h^p} k\left(\left\|\frac{x^s}{h_s}\right\|^2\right) k\left(\left\|\frac{x^r}{h^r}\right\|^2\right) \tag{11}$$

Among them, x^s represents the spatial feature component, x^r represents the color feature component, $k(x)$ represents the common representation function applied in the two feature domains, h_s and h_r represent the nuclear bandwidth, and c represents the normalization constant.

3) Mean shift process

The mean shift step calculation iteration is performed on the sampled pixels x_i, $i = 1, ..., n$. The ultimate goal is to find the mode points of each cluster set and to use the point set z_i to save all the mode points.

4) Combination and assignment

We combine the spatial feature distances of any two points in all mode points that are less than h_s and z_i and whose color gamut feature distance is less than h_r as a cluster,

and finally we determine the number of cluster sets $\{C_p\}_{p=1,\ldots,m}$. By assigning the same pixel value to each category in the cluster set, the final result of image segmentation is obtained.

2. Edge detection algorithms based on confidence

Traditional edge detection algorithms mainly use the gradient amplitude information of pixels, such as the Sobel algorithm and the Canny algorithm (Canny 1986), etc., which has poor ability to detect weak edges, and easily introduces false edges while detecting. The edge detection method based on confidence (Meer and Georgescu 2001) makes full use of the gradient phase information of the pixel. The standard edge template is determined by the gradient phase of the field center, and the normalized data vector and the absolute value of the standard template correlation coefficient are taken as the confidence of the edge. The structural information of the image in then used to determine whether the point is an edge in order to achieve the purpose of accurately detecting weak edges in the image.

2.1. Definition of confidence

Let w_1 and w_2 be the vectors of the two differential operator templates, these form a hyperplane $R^{(2m+1)^2}$, $w_\perp$ is the orthogonal component, a is the unit vector, and the projection of a on the hyperplane $R^{(2m+1)^2}$ formed by w_1 and w_2 is P_a. According to the definition of w_1 and w_2, the direction of P_a on the hyperplane is a gradient operator. The edge template in the direction of $\hat{\theta}$ is t. Therefore, the edge confidence can be defined as the inner product of the template vector and the vector window in the image, as shown in Equation (12).

$$\eta = |t^T a| \tag{12}$$

Among them, t and a are unit vectors, and η is the absolute value of the correlation coefficient between the standardized vector and the template parameter. The edge confidence is calculated using image information and standard template information. The angle $\hat{\theta}$ between t and a is independent of η. Therefore, η implements the independent estimation of the hypothetical edge model within the process window.

2.2. Edge detection implementation method

2.2.1. Non-maximum suppression

Let $\hat{g}_{[1]} < \ldots < g_{[k]} < g_{[k+1]} < \ldots < g_{[N]}$ be an ordered set sorted by different gradient-size values. For each pixel, its edge intensity $\hat{g}_{[k]}$ can be represented by its probability, as shown in Equation (13).

$$\rho_k = \text{Prob}\left|\hat{g} < \hat{g}_{[k]}\right| \tag{13}$$

ρ^k is the percentage of the cumulative gradient intensity distribution. Therefore, the context information of the ρ – η picture can be used to define non-maximum suppression and hysteresis threshold.

Let $f(\rho,\eta) = 0$ represent the invisible equation of the curve in the ρ – η plane. For any point (ρ_0,η_0), $f(\rho_0,\eta_0)$ can be used as the algebraic distance from (ρ_0,η_0) to curve $f(\rho,\eta) = 0$. The algebraic distance of all points on the curve is zero. According to the algebraic distance, the graph of plane ρ – η can be divided into two parts. Let $f(\rho,\eta) > f(\rho_P,\eta_P)$ represent the distance as positive, otherwise it represents the distance as negative.

2.2.2. Hysteresis threshold processing

During the execution of the hysteresis threshold step, two discriminant equation curves $f^{(L)}(\rho,\eta) = 0$ and $f^{(H)}(\rho,\eta) = 0$ are set in the figure of the ρ – η plane. These divide a picture of the ρ – η plane into three regions. Among them, the points that fall outside the decision boundary of $f^{(H)}(\rho,\eta) = 0$, marked as P_H, can be directly judged as edge points; the pixels that fall on the inside of the decision boundary of $f^{(L)}(\rho,\eta) = 0$ can be removed as non-edge points, recorded as P_L; the pixels that fall in the middle of the two equation curves. The point is the target of the hysteresis threshold step and is denoted as P_M. When the neighboring point around P_M is an edge point, it is judged that the pixel point is also an edge point (Rui and Jintao 2020).

2.3. Edge detection parameter selection

As far as we know, the final detection result based on the confidence edge detection algorithm is determined by the size of the template of window w and the high and low threshold decision boundary. The size of the template of the window w is different, the distribution of the $f(\rho,\eta)$ curve equation in the figure of the ρ – η plane is different, and the result of the edge judgment using the decision boundary is also different. The larger the template, the larger the overall calculation amount, so in practical applications, only window templates below the 7 × 7 – pixel size are used for edge detection on the actual image. The decision boundary

equation in the figure of plane ρ – η usually adopts the form of an ellipse line, of course, other curve forms can also meet the requirements.

2.4. Edge detection procedure based on confidence

The above-mentioned process analysis and introduction is summarized and organized into a flowchart, as shown in Figure 1.

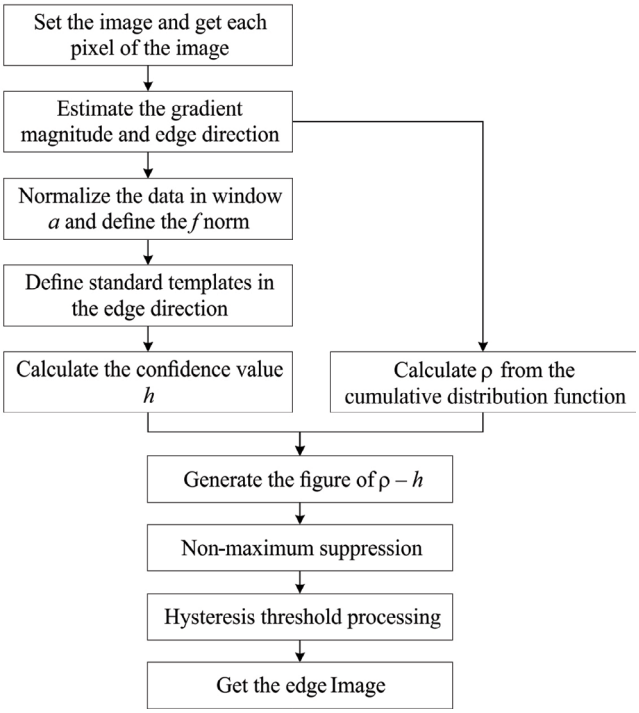

Fig. 1. Edge detection flow

Rys. 1. Schemat wykrywania krawędzi

3. Ore image segmentation method based on the fusion of the confidence edge algorithm and the mean shift algorithm

3.1. Introduction to the fusion algorithm procedure

Since this article is mainly applied to the problem of ore identification and extraction, considering that if only the initial image segmentation is used to extract the ore, over-

-segmentation may exist. Over-segmentation mainly refers to the division of an entire region into multiple small parts. In terms of ore identification, the ore region or the ore pile region is divided into multiple small parts which do not appear as a whole region. The improved image segmentation method proposed in this paper based on the fusion of the confidence edge detection algorithm and the mean shift image segmentation algorithm can combine the respective advantages of the two methods. Appropriate threshold parameters should be used to perform the initially segmentation in order to obtain lots of smaller image regions, and then the confidence edge detection algorithm should be used to extract all the edges around the ore region. The last step is to calculate the distribution of the peripheral edge points between each area and the surrounding adjacent segmentation area. When the proportion of the edge points of the adjacent area boundary is less than the specified threshold, two regions should be merged. The fusion method flow is shown in Figure 2.

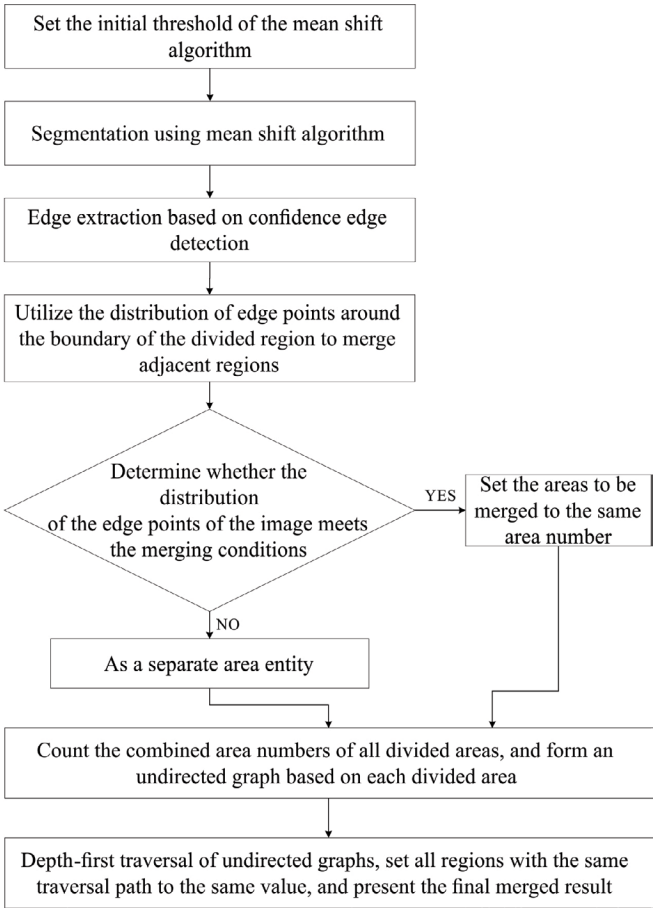

Fig. 2. Adjacent segmentation region merging based on the confidence edge detection method

Rys. 2. Proces ponownego łączenia sąsiednich obszarów segmentacji w oparciu o metodę wykrywania krawędzi ufności

3.2. Algorithm implementation procedure

1) Feature acquisition

Convert the RGB color space to the LUV color space, and combine the image space characteristics and color characteristics to form a feature vector $x = (x^r, x^s) = (x^*, y^*, L, U, V)$.

2) Mean shift process

Calculate the mean shift of all pixels and the sum of the color vectors of all sample points relative to the center point, and move the center point of the iterative space to the end of the vector, and then calculate the vector sum of all points in the spherical space again; this will iterate until the end of the vector sum obtained in the last space sphere is the center point P_n of the space sphere and the whole procedure ends. The color value of the corresponding initial origin P_0 on the output image *dst* is updated to the color value of the end point P_n based on iteration, then the color average shift of one sample point is completed. After traversing all the points, the entire mean shift image segmentation process is completed. Finally, $\{z_i\}_{i=1,\ldots,k}$ is formed as a cluster mode point set, and the region obtained by image segmentation is numbered as $\{0, \ldots, n\}$.

3) Edge point detection

Set the gradient operator and length threshold parameters in the edge detection algorithm and calculate the value of ρ and the confidence η of each pixel and finally use non-maximum suppression and the hysteresis threshold to calculate the edge points.

4) Merge region

Count the number of boundary points between each area and the surrounding adjacent areas, and set the total number of boundary points as n_w, count the number of surrounding points around the boundary point as n_e and finally calculate the proportion p_r of the surrounding edge points to the total number of boundaries, as shown in Formula (14).

$$p_r = n_e / n_w \tag{14}$$

Set the merge threshold t_c. When $p_r > t_c$, merge the two areas, set the region label to the same value and form an undirected graph of the area. The depth-first traversal algorithm is used to traverse the area numbers of the undirected graph and merge the areas. When $p_r > t_c$, do not merge two adjacent regions.

4. Experimental results and analysis

4.1. Parameter selection

This section mainly discusses the segmentation and extraction results of the ore image on the grid sieve under the metal mine after the methods described in the above sections

have been performed. Figure 3 shows ore images in two scenes. From left to right, they are the original RGB image, the initial segmentation image of the mean shift algorithm, the optimized segmentation image based on the fusion of the edge detection method with the confidence and mean shift algorithm, along with add edge point results based on confidence edge detection on the optimized segmented image. During this experiment, the size of the parameter window used by the mean shift algorithm is set as 7 × 7, the color space bandwidth as 2.5, and the minimum clustering region threshold (MinRegion) as 20. The gradient operator is set based on the confidence edge detection algorithm as 2 × 2, and the length threshold parameter is set as 10.

4.2. Results display and analysis

The following two sets of images show the result of edge detection based on confidence, the segmentation result of the mean shift algorithm, and the final result after the two algorithms merged.

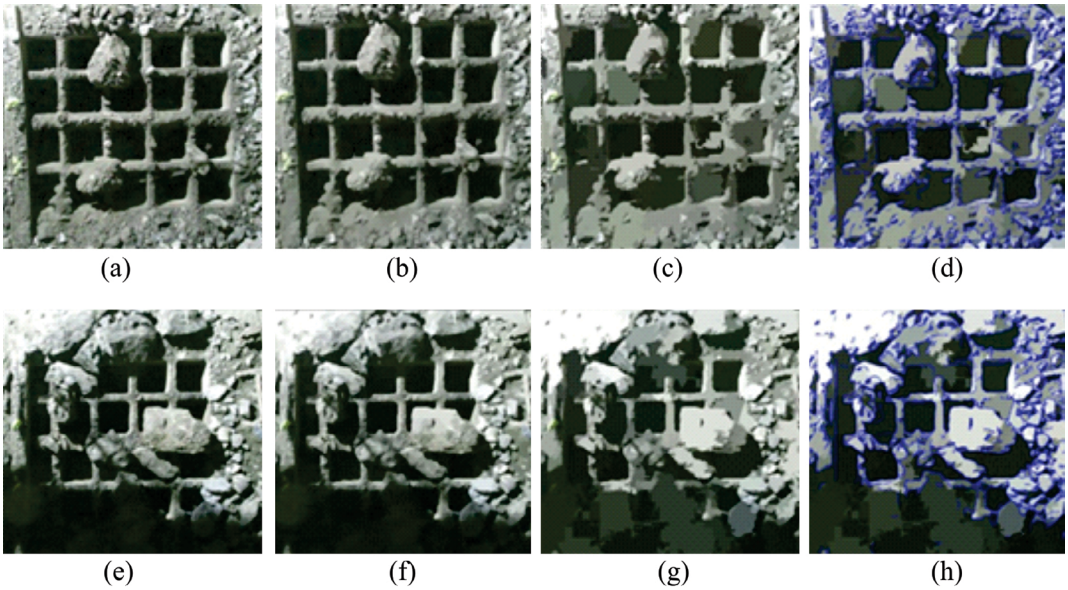

Fig. 3. Segmentation results of different ore scenes after using various algorithms
(a) (e) the original image; (b) (f) the initial segmentation result of the mean shift algorithm;
(c) (g) the segmentation result fused by the edge detection based on the confidence and the mean shift algorithm;
(d) (h) superimposed edge detection results on the final segmented image

Rys. 3. Wyniki segmentacji innych obrazów rudy po zastosowaniu różnych algorytmów
(a) (e) oryginalny obraz; (b) (f) początkowy wynik segmentacji algorytmu zmiany średniej;
(c) (g) wynik segmentacji połączony przez wykrywanie krawędzi w oparciu o poziom ufności i algorytm zmiany średniej; (d) (h) detekcja nałożonych krawędzi daje końcowy segmentowany obraz

According to the analysis of the two scene images in Figure 3, the initial segmentation results (b) (f) of the mean shift algorithm obviously show that the entire ore area is divided into multiple small areas under the observation of the human eye, which results in the over-segmentation phenomenon. However, after the edge detection method based on confidence, when there is a large proportion of edge points around the ore region, the adjacent areas are merged. While there is a smaller proportion of edge point distribution around the ore region, the algorithm does not take merging into account. In the end, there are still situations in which merging is not complete under human observation. In this case, the idea of this article is not to adjust the edge length threshold parameter more strictlyor to solve over-segmenting problem, therefore the problem that the area does not belong to a whole ore area, which is forcibly divided into one area, and results in the offset of the subsequent crushing position, does not exist.

From the analysis of the two typical ore scene images in Figure 4, it can be seen that there is obvious over-segmentation in (a) and (e) after simply using the mean shift algorithm, this means that the whole stone is divided into multiple small areas, such as (a). The area on both sides of the red framed area should be divided into pieces of ore. Since there are no edge points in the red box in (b), the fusion algorithm in this paper is used to merge the two regions in the red box in (a). The fusion result of (a) is (c) and (d); the two red boxes in the

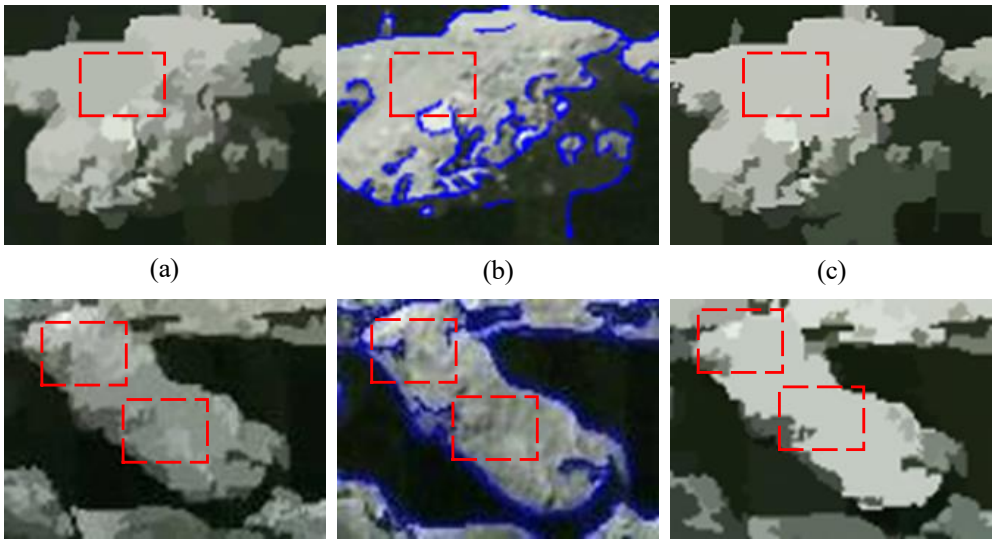

Fig. 4. The display of ore segmentation results in typical scenarios
(a) (e) initial segmentation result of mean shift algorithm; (b) (f) the result of applying edge detection based on confidence to the original image; (c) (g) the result of fusion algorithm and edge points display

Rys. 4. Prezentacja wyników segmentacji rudy w typowych scenariuszach
(a) (d) początkowy wynik segmentacji algorytmu zmiany średniej; (b) (e) wynik zastosowania wykrywania krawędzi w oparciu o pewność oryginalnego obrazu; (c) (f) zaproponowany algorytm fuzji zawarty w końcowym obrazie podzielonym na segmenty

picture should be divided into a single piece of ore. Because in (e) there are no edge points in the two red boxes of the same area in the picture, the two areas around the red box should be merged to get the final ore segmentation result (f).

In this research, we estimate the accuracy of segmentation with the following indicator: the segmentation region count and the proportion of the maximum region within actual ore regions. We compare above indicators under different algorithms: the common mean-shift algorithm, the watershed algorithm, the fusion of mean-shift algorithm and embedded confidence edge detection.

Firstly, we show segmentation results of the different algorithms. In Figure 5a–e, the first column image is the original image, the second column image is the segmentation result acquired by the watershed algorithm, the third column image is the segmentation result by the mean-shift, and the fourth column image is the segmentation result acquired by the fusion of the embedded confidence edge detection and the mean-shift algorithm. We can see that the watershed algorithm cannot segment the ore region and the background effectively – the segmented ore region wrongly contains the background regions. The reason causes the phenomenon of the watershed to be sensitive to the noise and the discontinuity of the object surface.

The mean-shift method can also cause over-segmentation problems– we can see this from the third column of Figure 5a–e. When the kernel window size is small, ore is segmented to numerous regions, and when the color bandwidth is small, the over-segmentation problem also appears. By contrast, ore can mix with the background when the color bandwidth is set to a large value.

Fusion of embedded confidence edge detection and mean-shift is based on small color bandwidth and kernel window bandwidth. It can merge surrounding small regions and do not mix the ore region with the background region. From the fourth column, we can see the final merged region size is nearly equal to the actual ore size.

Secondly, we calculate the total pixel count of regions based on different algorithms, and then get the segmented result proportion of an actual ore region. In Figure 6, we have manually labeled the boundary of the ore region of interest. Table 1, presents the segmented region pixel count and the proportion of the actual region according to the maximum regions that intersect with the actual region.

In Table 1, we use WS, MS, EDMS to represent different algorithm – WS represents the watershed algorithm, MS represents the mean-shift algorithm, and EDMS represents the fusion of embedded confidence edge detection and the mean-shift. The region index is the region number from the five images above; image one contains two regions, image two contains two regions, image three contains two regions, image four and image five contain six regions in total.

As we can see from Table 1, the mean-shift algorithm does not perform well in all scenarios – the proportion of the actual region is mostly under fifty percentage. The watershed algorithm performs better than the mean-shift, but when noise and discontinuity happens, it does not yield a satisfactory segmentation result. Lastly, when the mean-shift combines

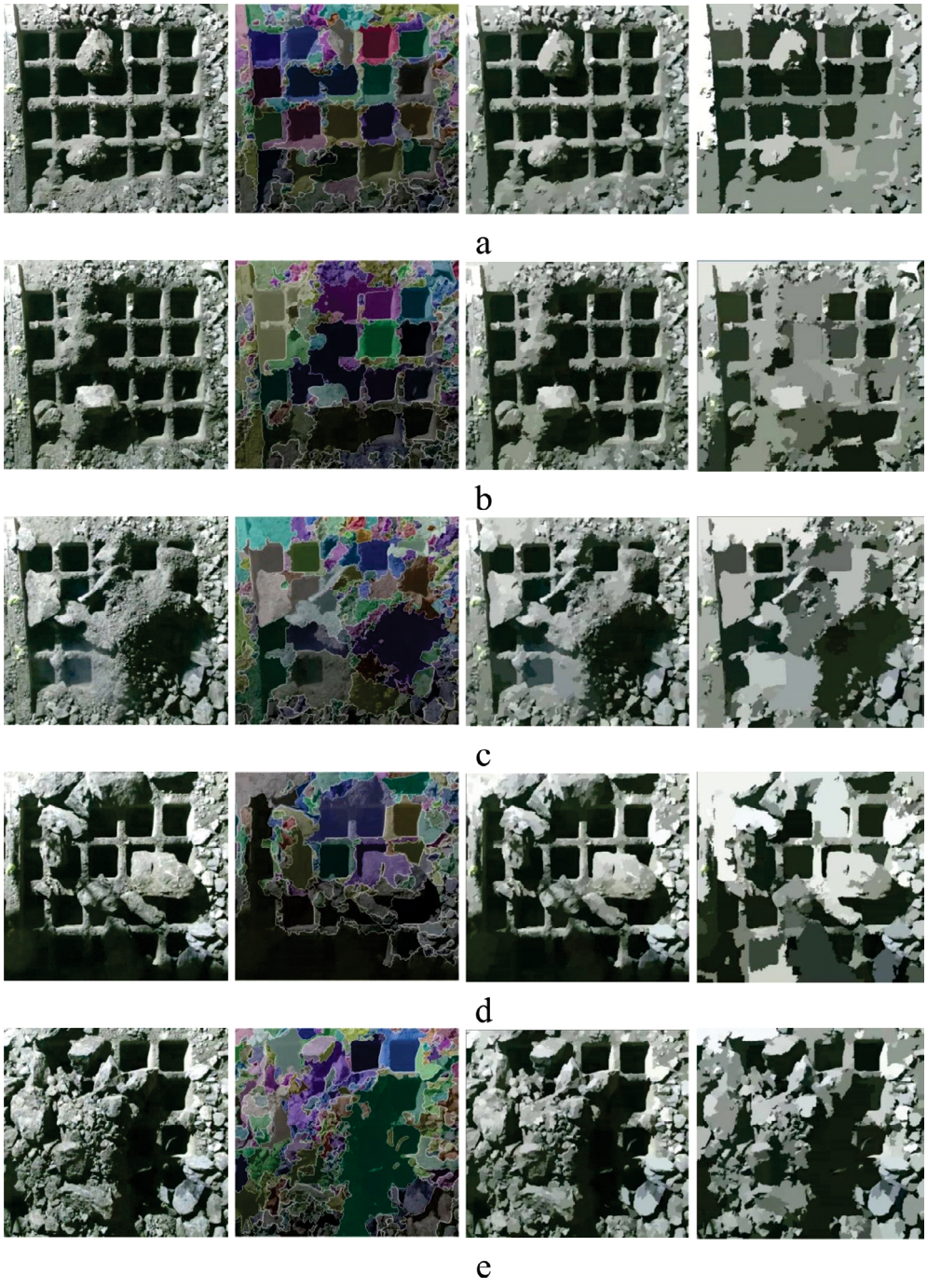

Fig. 5. Segmented result of different algorithms

Rys. 5. Segmentowany wynik różnych algorytmów

Fig. 6. Manually labeled boundary of interest of the ore region with blue lines

Rys. 6. Ręcznie oznaczona niebieskimi liniami granica zainteresowania obszarem rudy

Table 1. The quantitative estimation to different segmentation algorithm

Tabela 1. Estymacja ilościowa dla różnych algorytmów segmentacji

Region index	Methods	Actual region count	Segmented region count	Proportion of actual region
1-1	WS MS EDMS	5,913	3,287 1,923 4,879	55.58% 32.52% 82.51%
1-2	WS MS EDMS	3,968	2,146 1,567 3,264	54.08% 39.49% 82.25%
2-1	WS MS EDMS	11,704	3,753 3,479 8,642	32.06% 29.72% 73.83%
2-2	WS MS EDMS	5,503	3,351 4,032 4,367	60.89% 73.26% 79.35%
3-1	WS MS EDMS	7,313	9,798 3,015 6,234	136.44% 41.22% 85.24%
3-2	WS MS EDMS	2,554	1,848 987 2,097	72.35% 38.64% 82.10%
4-1	WS MS EDMS	4,338	2,848 1,684 3,491	65.65% 38.81% 80.47%
4-2	WS MS EDMS	4,076	3,045 1,783 3,476	74.70% 43.74% 85.27%
4-3	WS MS EDMS	10,509	9,548 5,639 8,015	90.85% 53.65% 76.26%
5-1	WS MS EDMS	2,292	1,280 1,458 1,640	55.84% 63.61% 71.55%
5-2	WS MS EDMS	6,786	3,534 2,159 5,367	52.07% 31.81% 79.08%
5-3	WS MS EDMS	3,175	1,908 1,347 2,379	60.09% 42.42% 74.92%

with the embedded confidence edge detection algorithm, the segmentation results are largely improved based on an effective merging strategy.

In summary, compared to image segmentation algorithms that only use edge detection and mean shift algorithms, the fusion algorithm proposed in this paper overcomes the shortcomings of the above two algorithms and better completes the image segmentation of ore and ore regions. According to quantitative analysis of the existing algorithms applied in the above discussion, we can draw the conclusion that, in this research, we can accurately locate ore regions by fusion of embedded confidence edge detection and mean-shift, and this method can then be used in ore size property estimation combined with other relevant devices, which would be useful in grinding and cracking processes in the future.

Conclusion

The main work of this paper is to apply the optimized image segmentation algorithm based on the confidence-based edge detection algorithm and the mean shift clustering segmentation algorithm to the ore and ore region image segmentation. Because the ore texture features and color features are very similar, in the process of image segmentation, ore images often have over-segmentation phenomena if only edge features or clustering are used for segmentation. Therefore, the idea of this paper is to combine these two to optimize the segmentation method to solve the over-segmentation issues. The ore of the scene image is effectively segmented in a way that is close to human visual observations.

From the analysis of the actual scene experiment results, without the edge detection algorithm based on confidence, the ore area is very similar because of the color and texture characteristics, and the color bandwidth must be small enough to more accurately segment the ore area. When the color bandwidth is set to a small value, over-segmentation occurs, which is not beneficial to the subsequent calculation of the geometric parameters of the overall ore. The edge detection algorithm based on confidence can better solve the over-segmentation problem. The adopted idea is to count the edge points that exist around the boundary of the smaller segmented area. When the edge point distribution does not exceed a certain proportion, the two areas are merged, otherwise, no merging is performed. From the experimental results, the over-segmentation situation has been significantly improved, and the final segmentation area presented by the algorithm is close to the real ore area.

This work was jointly supported by the National Key Research and Development Program of China (No. 2018YFC0604403) and the Scientific Research Fund of BGRIMM Technology Group (No. 02-2036-WG).

REFERENCES

Boyuan et al. 2021 – Boyuan, M., Shufang, J., Dou, Y., Haokai, S. and Xiaojuan, B. 2021. Image segmentation metric and its application in the analysis of microscopic image. *Chinese Journal of Engineering* 43, pp. 137–149. DOI: 10.13374/j.issn2095-9389.2020.05.28.002.

Canny, J. 1986. A Computational Approach to Edge Detection. *IEEE Transactions on Pattern Analysis and Machine Intelligence*, PAMI-8, pp. 679–698.

Cheng, Y. 1995. Mean shift, mode seeking, and clustering. *IEEE Transactions on Pattern Analysis and Machine Intelligence* 17, pp. 790–799.

Comaniciu, D. and Meer, P. 1997. Robust analysis of feature spaces: color image segmentation. *Conference on Computer Vision and Pattern Recognition*.

Comaniciu, D. and Meer, P. 1999. Mean shift analysis and applications. *Proceedings of the seventh IEEE international conference on computer vision*. IEEE, pp. 1197–1203.

Comaniciu, D. and Meer, P. 2002. Mean Shift: A Robust Approach Toward Feature Space Analysis. *IEEE Transactions on Pattern Analysis and Machine Intelligence* 24, pp. 603–619. DOI: 10.1109/34.1000236.

Georgescu ae al. 2003 – Georgescu, B., Shimshoni, I. and Meer, P. 2003. Mean shift based clustering in high dimensions: A texture classification example. Computer Vision, IEEE International Conference on, 2003. *IEEE Computer Society*, pp. 456–456.

Lin et al. 2005 – Lin, K., Wu, J. and Xu, L. 2005. A survey on color image segmentation techniques. *Journal of Image and Graphics* 10, pp. 1–10. DOI: 10.1007/s41095-020-0177-5.

Liu et al. 2020 – Liu, X., Zhang, Y., Jing, H., Wang, L. and Zhao, S. 2020. Ore image segmentation method using U-Net and Res_Unet convolutional networks. *RSC Advances* 10, pp. 9396–9406. DOI: 10.1039/C9RA05877J.

Meer, P. and Georgescu, B. 2001. Edge Detection with Embedded Confidence. *IEEE Transactions on Pattern Analysis and Machine Intelligence* 23(12), pp. 1351–1365.

Qin, C. and Liu, Q. 2015. Image segmentation of pellets based on improved watershed algorithm. *Journal of Wuhan University of ence and Technology*, pp. 56–59.

Rui, Z. and Jintao, L. 2020. A Survey on Algorithm Research of Scene Parsing Based on Deep Learning. *Journal of Computer Research and Development* 57(4), pp. 859–875. DOI: 10.7544/issn1000-1239.2020.20190513.

Skarbek, W. and Koschan, A. 1994. *Colour Image Segmentation: A Survey.*

Xiang-Ru et al. 2005 – Xiang-Ru, L.I., Fu-Chao, W.U. and Zhan-Yi, H.U. 2005. Convergence of a mean shift algorithm. *Journal of Software* 16(3), pp. 365–374.

Xu et al. 2019 – Xu, W., Zhang, G., Jiang, Y. and Chen, L. 2019. Ore segmentation method by Bi-window OTSU based on binomial distribution. *Nonferrous Metals (Mining Section)* 71, pp. 101–107. DOI: 10.3969/j.issn.1671-4172.2019.03.021.

Ying et al. 2005 – Ying, L., Song, H.N. and Yi, S.U. 2005. An Approach to Edge Detection Based on Confidence. *Computer Simulation* 22, pp. 195–196.

IMAGE SEGMENTATION METHOD OF MINE PASS SOIL AND ORE BASED ON THE FUSION OF THE CONFIDENCE EDGE DETECTION ALGORITHM AND MEAN SHIFT ALGORITHM

Keywords

edge detection, confidence, mean shift algorithm, image segmentation

Abstract

In the execution of edge detection algorithms and clustering algorithms to segment image containing ore and soil, ore images with very similar textural features cannot be segmented effectively when the two algorithms are used alone. This paper proposes a novel image segmentation method based on the fusion of a confidence edge detection algorithm and a mean shift algorithm, which integrates image color, texture and spatial features. On the basis of the initial segmentation results obtained by the mean shift segmentation algorithm, the edge information of the image is extracted by using the edge detection algorithm based on the confidence degree, and the edge detection results are applied to the initial segmentation region results to optimize and merge the ore or pile belonging to the same region. The experimental results show that this method can successfully overcome the shortcomings of the respective algorithm and has a better segmentation results for the ore, which effectively solves the problem of over segmentation.

METODA SEGMENTACJI OBRAZU GLEBY I RUDY W OPARCIU O POŁĄCZENIE ALGORYTMU WYKRYWANIA KRAWĘDZI UFNOŚCI I ALGORYTMU ZMIANY ŚREDNIEJ

Słowa kluczowe

wykrywanie krawędzi, ufność, algorytm zmiany średniej, segmentacja obrazu

Streszczenie

W procesie algorytmu wykrywania krawędzi ufności i algorytmu grupowania do segmentacji obrazu zawierającego rudę i glebę, obraz rudy o bardzo podobnych cechach tekstury nie może być skutecznie segmentowany, gdy oba algorytmy są używane osobno. W pracy zaproponowano nowatorską metodę segmentacji obrazu opartą na połączeniu algorytmu wykrywania krawędzi ufności i algorytmu zmiany średniej, który integruje kolor, teksturę i cechy przestrzenne obrazu. Na podstawie wstępnych wyników segmentacji uzyskanych przez algorytm segmentacji zmiany średniej informacja o krawędziach oryginalnego obrazu jest wyodrębniana za pomocą algorytmu wykrywania krawędzi opartego na stopniu ufności, a otrzymane wyniki są stosowane do początkowych wyników segmentacji obszaru w celu optymalizacji i scalenia rudy lub gleby należących do tego samego obszaru. Wyniki eksperymentalne pokazują, że metoda ta może skutecznie przezwyciężyć wady odpowiedniego algorytmu i daje lepsze wyniki segmentacji dla rudy, co dobrze rozwiązuje problem nadmiernej segmentacji.